

# Gate Drive Power Supply for On-board Marx Circuit Using only Charging Path of Marx Capacitor

Keisuke Kusaka  
Dept. of Electrical, Electronics, and  
Information Engineering  
Nagaoka University of Technology  
Nagaoka, Japan  
kusaka@vos.nagaokaut.ac.jp

Yosuke Ouchi  
Dept. of Electrical, Electronics, and  
Information Engineering  
Nagaoka University of Technology  
Nagaoka, Japan  
yosuke0113@stn.nagaokaut.ac.jp

Jun-ichi Itoh  
Dept. of Electrical, Electronics, and  
Information Engineering  
Nagaoka University of Technology  
Nagaoka, Japan  
itoh@vos.nagaokaut.ac.jp

**Abstract**— This paper proposes a gate drive power supply method for a Marx circuit with high-voltage output. The conventional gate drive power supply method has a disadvantage that the gate drive requires expensive and huge DC-DC converters to secure the insulation distance because of the high-voltage operation of the Marx circuit. In this paper, the gate drive power is supplied through a transformer inserted into the charging path of the Marx capacitor in order to overcome these problems. The inserted transformer also plays a role in suppressing the rush current during the charging operation of the Marx circuit. The proposed power supply method reduces the gate circuit volume and improves efficiency. In this paper, the parameter design for obtaining the desired gate drive power is explained. Then, it is verified that a driving power of 1 W or more is obtained by simulation and prototype. The charging current flowing during charging is suppressed by 75%, and the loss during charging was reduced.

**Keywords**—Marx circuit, Gate drive circuit, Power supply method,

## I. INTRODUCTION

In recent years, regulations on NO<sub>x</sub> gas emissions have been tightened in each country to prevent global warming. The popularization of EVs, which has no emission of NO<sub>x</sub> gas, is one of the solutions against global warming. However, vehicles with gasoline or diesel engines are still mainstream since the energy density of batteries is lower than fossil fuels. For gasoline or diesel engines, NO<sub>x</sub> emission reduction is essential to comply with the regulations. In order to reduce the NO<sub>x</sub> emission, a catalyst has been used. However, it will not be enough to comply with the regulations, which will become stricter in the future.

The Marx circuit, as a pulse power source, has been widely studied for medical purposes, sterilization, and NO<sub>x</sub> reduction applications [1-15]. The plasma generated by the Marx circuit produces ozone. The NO<sub>x</sub> gas emission is suppressed by reacting the ozone generated by the Marx circuit with the NO<sub>x</sub> gas. For automotive applications, the Marx circuit should be mounted on the vehicle.

This paper focuses on a pulse power supply for an exhaust gas treatment system for vehicles with a diesel engine. As requirements for ozonizers, lighter weight, smaller size, and higher efficiency are required. However, rush current occurs during charging. The heat occurs by the rush current prevents miniaturization. [2]. The rush current occurs in the circuit when the capacitor in the Marx circuit discharges and recharges. The equivalent circuit of the Marx circuit during the charging operation is a series circuit of the input power supply, the capacitors connected in multiple stages, and the

on-resistance of the power devices. Therefore, the power device may be damaged due to an excessive rush current. In particular, improving the efficiency of the Marx circuit by using SiC or GaN devices is expected as a recent trend. However, the reduced on-resistance of the device will increase the rush current.

There are some literatures that employs a current source as the input power supply for a Marx circuit to suppress rush current or adding resistance and inductance to the path [3-11]. However, the rush current occurs in the circuit due to the voltage fluctuation of the capacitors on each stage. The additional components must increase the volume of the Marx circuit. However, rush current occurs between each stage due to variations in the capacitor capacitance of each stage. Therefore, the suppression of rush current is not sufficient in [3-11].

Regarding the gate drive circuit of the Marx circuit, the Marx circuit uses three power devices in each stage. The on-board Marx circuit needs 10 or more stages. All that device requires expensive and large isolated DC-DC converters. Therefore, the gate circuit area must be large. In order to reduce the area of the gate drive circuit of the Marx circuit, a method of transmitting the gate signal and the drive power at the same time has been studied [12-13]. The system is useful because the signals of the Marx circuit are synchronized. However, since power is supplied to multiple devices, there are concerns about power imbalance. In [14-15], a method has been proposed in which gate drive power is supplied from the main circuit using a transformer. The use of this method in the Marx circuit has the effect of suppressing the rush current. Therefore, The gate circuit is miniaturized.[16-18]

In this paper, the circuit configuration for the power supply of the gate driver using the transformer in the charging path of the Marx circuit is proposed. The rush current is suppressed by the proposed power supply method. Since the current flowing through the inserted transformer is used to supply power to the gate drive unit (GDU), the number of isolated DC-DC converters for gate drivers is reduced. This features contribute to miniaturize the Marx circuit. Further, it is possible to suppress the rush current between the capacitors connected in multiple stages, which is a problem in the Marx circuit.

## II. GATE DRIVE POWER SUPPLY FOR MARX CIRCUIT

### A. Circuit Configuration

Figure 1 shows the operation of the Marx circuit with a transformer for an auxiliary power supply and the Marx circuit.

The first stage of the Marx circuit has switches  $S_1$ ,  $S_2$ , and  $S_6$ , and  $C_1$  Marx capacitors. Supplied power circuit shows the configuration of the GDU in the proposed power supply method in fig. 2. The Marx circuit is a stack of stages with the same structure. In this paper, the two-stage Marx circuit is explained for simplicity, however, the proposed power supply method will be applied to also a Marx circuit with a higher number of stages. The auxiliary power supply supplies power to the gate drive circuit. The two modes of the Marx circuit: discharging mode and charging mode, are explained. In the discharging mode, the switches  $S_2$  and  $S_4$  are turns on. Then, Marx capacitors are connected in series, and a high voltage with high  $dv/dt$  is applied to the load. During the charging mode, the switches  $S_1$ ,  $S_3$ ,  $S_5$ , and  $S_6$  turns on. The Marx capacitors are connected in parallel, and the Marx capacitors are charged. In order to obtain high  $dv/dt$ , the Marx circuit should not have an inductance in the discharging path. However, in order to suppress the rush current, inductance is necessary for the charging path. The proposed power supply method has a transformer inserted into the charging path, so it does not affect the discharging operation. During the charging mode, the current flows through the inserted primary coil. A magnetic flux is generated by the current flowing on the primary coil, and the magnetic flux is coupled to the secondary coil to supply power.

Figure 2 shows an equivalent circuit of the Marx circuit and the gate drive supply during the charging operation. In this paper, analysis and simulation are performed using the circuit shown in Fig. 2. The equivalent circuit consists of a T-type equivalent circuit of the transformer, a rectifier, and a Marx capacitor  $C_1$ . The resistance  $R$  is the sum of the on-resistance of the MOSFETs and the wiring resistance of the charging current path. In this study, the gate drive voltage is constant at 16 V. The analysis is performed by assuming the output voltage of the rectifier is constant for simplicity. The Marx capacitor  $C_1$  is discharged from the input voltage during the discharge operation ( $t < 0$ ). The transformer is designed by assuming that the voltage of the Marx capacitors drops by  $\Delta V$  due to the discharging operation. At  $t = 0$ , the charging operation starts by turning on the switch. The current flows through the primary winding of the transformer and the Marx capacitor. During the charging operation, the secondary current flows into the rectifier.

### B. Transformer design

In this section, the transformer of the proposed power supply method is designed. First, the power applied to the secondary side is expressed as (1).

$$P_{out} = f_{sw} V_{out} \int i_{2(t)} dt \quad (1)$$

Where  $P_{out}$  is the supplied gate drive power,  $V_{out}$  is gate drive voltage of secondary side,  $f_{sw}$  is the switching frequency of the Marx circuit, and  $i_{2(t)}$  is the current on the secondary side. The discharge operation causes the voltage drop on the Marx capacitor  $C_1$ . In the charging operation, current flows in order to compensate for the voltage drop from the input power supply. Then, a current flow on the secondary side of the transformer. A GDU is connected to the secondary side of the transformer and clamped by the gate drive voltage. Therefore, the electric power obtained by one charging operation is the product of the gate drive voltage and the integrated value of the current flowing through the secondary side of the transformer. This operation occurs in every discharge cycle.

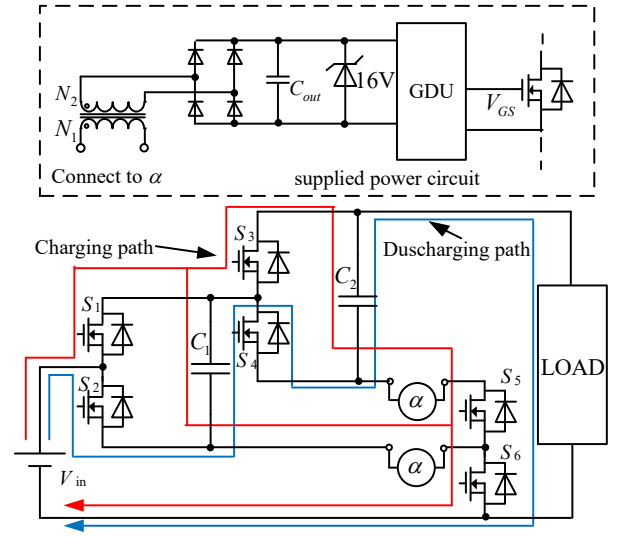


Fig. 1. Two stage Marx circuit and places to insert a transformer for obtaining gate drive power.

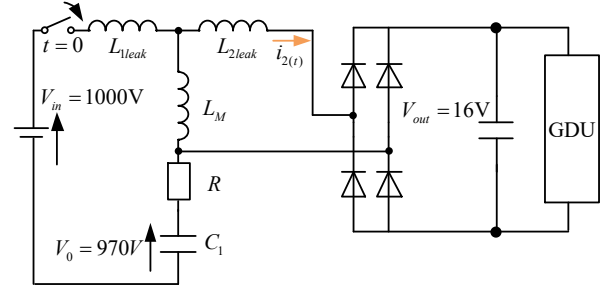


Fig. 2. Equivalent circuit during charging operation.

The switching frequency and the gate voltage are arbitrarily determined. The current flowing on the secondary side  $i_{2(t)}$  is given by the circuit equation expressed as (2),

$$i_{2(t)} = \frac{k(V_{in} - kV_{out} - V_0)}{\sqrt{\frac{\beta}{C_1} - \left(\frac{R}{2}\right)^2}} e^{-\frac{R}{2\beta}t} \sin \sqrt{\frac{1}{\beta C_1} - \left(\frac{R}{2\beta}\right)^2} t - \frac{kV_{out}}{L_{1leak} + L_M} t \quad (2)$$

$\beta = (L_{1leak} + L_M - kL_M)$  (3) where  $V_{in}$  is the input voltage,  $C_1$  is the Marx capacitor,  $V_0$  is the initial voltage of the Marx capacitor,  $R$  is the resistance component including wiring resistance and on-resistance of MOSFETs,  $k$  is the coupling coefficient of the transformer,  $L_{1leak}$  is the primary leakage inductance, and  $V_{out}$  is the DC voltage of the gate driver.

Figure 3 shows the waveform of the current flowing on the secondary side of the transformer of (2) in the red line. Also, the simplified current waveform shown in (4) is shown by a black line. The integral value of the current flowing on the secondary side of the transformer shown in the (1) is approximated to a triangle and shown in Fig. 3.

$$i_{2(t)} \approx \frac{k(V_{in} - kV_{out} - V_0)}{\sqrt{\frac{L_{1leak} + L_M - kL_M}{C_1} - \left(\frac{R}{2}\right)^2}} \sin \sqrt{\frac{1}{(L_{1leak} + L_M - kL_M)C_1}} t \quad (4)$$

Equation (2) is simplified as (3) due to the transformer design. For simplicity, the on-resistance of the MOSFETs are ignored. When the on-resistance is small enough to be ignored, the damping by the exponential function is ignored. The same applies to the part containing the on-resistance of the sine function term. Terms containing the on-resistance of the sine function is ignored. The third term of (1) is also ignored because the time interval of the current flowing during the charging period is much smaller than the first term. The integrated value of the current of (1) is obtained from the simplified current waveform of (3). At this time, the integrated value is calculated as the area of the triangle in Fig. 3.

Note that the time  $t_1$  and  $t_2$  are approximately calculated where the vibration term in (3) is zero and one. Therefore, it is expressed as shown below.

$$t_1 = \sqrt{(L_{1leak} + L_M - kL_M)C_1} \pi \quad (5)$$

$$t_2 = \frac{\sqrt{(L_{1leak} + L_M - kL_M)C_1} \pi}{2} \quad (6)$$

$$i_{\max} = \frac{k(V_{in} - kV_{out} - V_0)}{\sqrt{\frac{L_{1leak} + L_M - kL_M}{C_1} - \left(\frac{R}{2}\right)^2}} \quad (7)$$

According to the above equations, the primary and the secondary inductance should be designed with

$$L = \frac{C_1 R P^2}{(1 - k^2) \left[ 4P^2 - C_1 \left\{ f_{sw} V_{out} \pi k (V_{in} - kV_{out} - V_0) \right\}^2 \right]} \quad (8).$$

Note that there is an error in the output power due to the approximation, as shown in Fig. 3. Therefore, it is necessary to design the inductance with a margin, and it is necessary to increase the inductance in order to obtain higher power.

Finally, the voltage drop of the Marx capacitor in one discharging operation is described. The energy consumed by the Marx capacitor in one discharge operation is expressed as (9).

$$E_{drop} = \frac{P_{outmarx}}{N f_{sw}} \quad (9),$$

where  $P_{outmarx}$  is output power of the Marx circuit,  $E_{drop}$  is the power that the Marx capacitor of each stage is discharged by one discharge operation,  $N$  is the number of stages that make up the Marx circuit. Therefore, the voltage drop of the Marx capacitor is expressed by (10).

$$\frac{1}{2} C_{marx} V_{in}^2 - \frac{1}{2} C_{marx} V_{drop}^2 = E_{drop} \quad (10),$$

Where  $V_{drop}$  is the voltage of the Marx capacitor in one discharge operation. Therefore, the voltage after discharge is represented as (11),

$$V_{drop} = \sqrt{V_{in}^2 - \frac{2E_{drop}}{C_{marx}}} \quad (11),$$

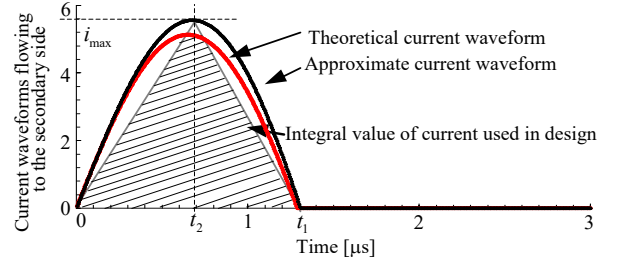


Fig. 3. Waveform approximating the current flowing in the secondary transformer.

Table. 1 Simulation conditions.

Variable	parameter	Value
$V_{in}$	Input voltage	1000 V
$V_0(t=0)$	Marx capacitor voltage	960 V
$C_1$	Marx capacitor capacity	0.22 $\mu$ F
$V_{out}$	Gate drive voltage	16 V
$L_1$	Primary inductance of transformer	10.5 $\mu$ H
$L_2$	Secondary inductance of transformer	10.5 $\mu$ H
$k$	Coupling coefficient	0.95
$R$	ON resistance	0.2 $\Omega$
$L_0$	Wiring inductance	100 nH

### III. EXPERIMENTAL VERIFICATION

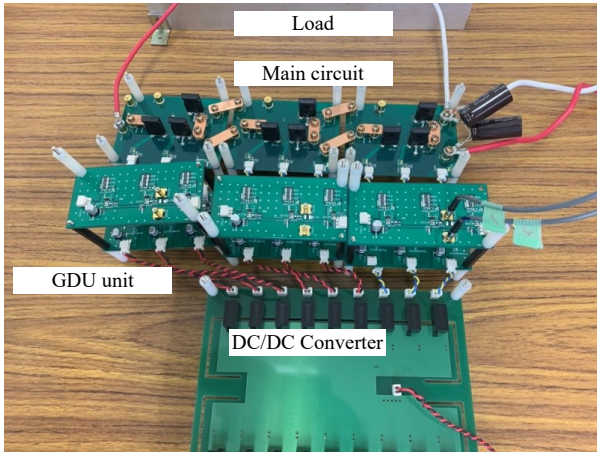
#### A. Suppression of rush current

In this section, the validity of simulations, theoretical formulas, and approximated formulas are verified using a prototype. First, the effect of suppressing the rush current is evaluated.

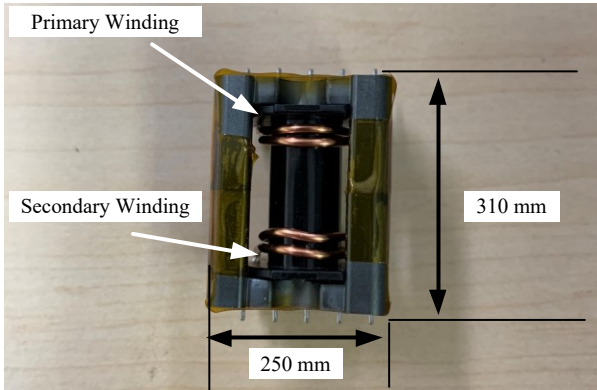
Figure 4 shows the prototype. Fig. 4(b) is the transformer for the gate drive power supply. This transformer is connected to  $\alpha$  in Fig. 1 to supply power to the gate circuit. In the experiment, the resistive load is used.

Table 2 shows the experimental conditions. The input voltage  $V_{in}$  is 100 V, and the voltage of the  $C_1$  capacitor drops by 30 V during the discharge mode. A primary inductance of the transformer must be 10  $\mu$ H or more, according to (7).

Figure 5 shows the effect of suppressing the rush current by the proposed power supply method. The charging current that flows in the first stage is indicated. Fig. 5(a) shows the charging current generated in the Marx circuit without a transformer for an auxiliary power supply in the charging path. The waveforms are the gate signal of  $S_1$  (charging signal of Marx circuit), charge current, and output voltage from the top. The charging current reaches to 40 A. When the Marx circuit consists of  $N$  stages,  $N$  times larger charging current for the capacitors on each stage will flow through  $S_1$  and  $S_6$  at the bottom. The charging current will exceed an absolute maximum rating of the power devices. The rush current must be suppressed for avoiding the circuit from the breakdown.



(a) Main Circuit



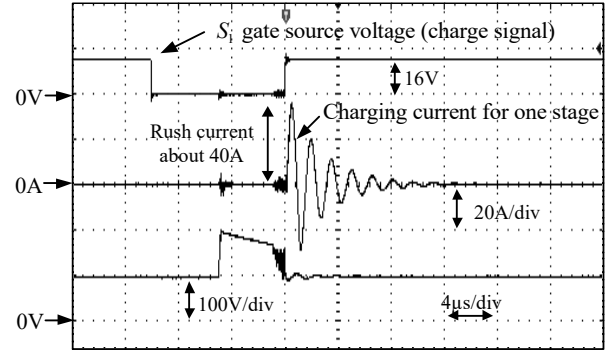
(b) Transformer for auxiliary power supply

Fig. 4. Prototype of Marx circuit and auxiliary power supply.

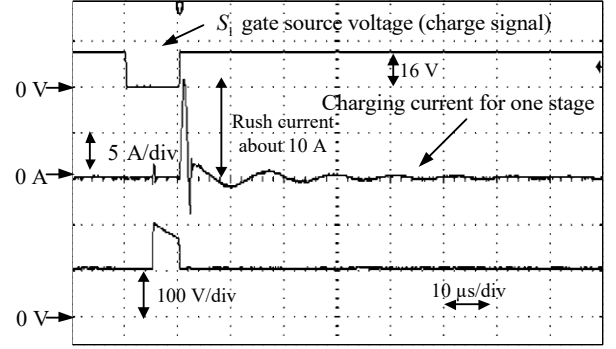
Table. 2. experimental condition.

Variable	parameter	Value
$V_{in}$	Input voltage	100 V
$V_0(t=0)$	Marx capacitor voltage	70 V
$C_1$	Marx capacitor capacity	0.22 $\mu\text{F}$
$V_{out}$	Gate drive voltage	16 V
$L_1$	Primary inductance of transformer	10.5 $\mu\text{H}$ , 23.7 $\mu\text{H}$
$L_2$	Secondary inductance of transformer	10.5 $\mu\text{H}$ , 23.7 $\mu\text{H}$
$k$	Coupling coefficient	0.95
$S_1 \sim S_6$	ON resistance	0.04 $\Omega$
	Continuous Drain Current	60 A
	Drain - Source Voltage	1200 V

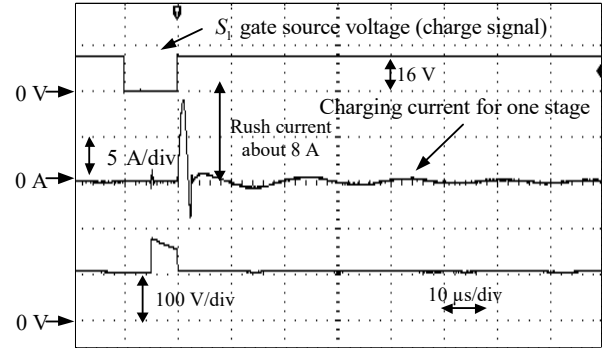
Figure 5(b) shows the waveforms when a transformer with a primary inductance of 10.5  $\mu\text{H}$  is inserted into the  $\alpha$  shown in Fig. 1. Similarly, Fig. 5(c) shows the waveform when a transformer with a primary inductance of 23.7  $\mu\text{H}$  is used. Experimental results show that the proposed power supply method suppresses the peak of the charging current to 10 A approximately. The charging current is suppressed to 75% using the proposed power supply method. Note that too much large primary inductance causes a problem in the operation of the Marx circuit. The charging period becomes longer when a



(a) Without a transformer



(b) 10.5  $\mu\text{H}$



(c) 23.7  $\mu\text{H}$

Fig. 5. Suppression effect of charging current by the proposed circuit.

transformer with a large primary inductance. The Marx capacitor  $C_1$  will not be fully charged during the charging period. It will affect the discharge operation, so there is a limitation on the primary inductance. In other words, the maximum power obtained from the Marx circuit is limited.

### B. Gate drive in the proposed power supply method

Figure 6 shows the operation waveforms of the proposed power supply method. In the experiment, the two transformers are tested. The primary inductances are 10.5  $\mu\text{H}$  or 23.7  $\mu\text{H}$ , the turn ratio is  $N_1 = N_2$ . The waveforms are the gate signal of  $S_1$  (charging signal of Marx circuit), the current through the secondary side of the transformer, output voltage, and the voltage of the Marx capacitor of the first stage. The peak current flowing on the secondary side of the transformer is about 8 A. The convergence time is about 1.6  $\mu\text{s}$ . This is consistent with the simulation shown in Fig. 3. During the discharge period, the proposed gate drive power supply does not affect the operation of the Marx circuit. In the current waveform of Fig. 6(b), the current peak is 8 A and it takes 2  $\mu\text{s}$  to converge. As inductance increases, more power is

delivered since the period of the oscillation term in (4) becomes slower, then the integrated value of the current increases. Note that the increase in the inductance has a limitation because a long oscillation period causes a problem that the next discharging operation will start before the primary current converges to zero. It means that the Marx circuit shuts the inductor current off at the start of discharging mode.

Figure 6 (c) shows the experimental waveform when the proposed circuit is operated in a steady state. The waveforms are the gate signal of  $S_6$ , the gate signal of  $S_1$ , the current waveform flowing to the secondary side during charging operation, and the load voltage from the top. The proposed gate drive system supplies the power to the switch  $S_1$ . From the experimental results, stable driving power is supplied during the charging operation.

Figure 7 shows the relationship between the primary inductance value of the transformer and the output power. In this graph, the inductance values of the primary side and the secondary side of the transformer are the same, and the turn ratio is  $N_1 = N_2$ . The validity of (8) is shown from the results of experiments and theoretical calculation. Fig. 7 shows that the supplied power increases as the inductance on the primary side and the secondary side increases. Moreover, since the power required for gate drive is about 1 W when the gate voltage is 16 V, the power required for gate drive is supplied by the proposed power supply method. However, if the gate voltage is 20 V, sufficient power cannot be obtained. This is explained by the decrease in the current peak shown at (7). Therefore, to obtain more power, it is necessary to increase the output of the Marx circuit and reduce the capacitor capacity and insert a transformer with a large primary inductance value.

Figure 8 shows operation waveforms when the input voltage  $V_{in}$  is increased from zero to 100 V. The DC voltage of the gate driver of  $S_1$  is automatically charged through the proposed system by the switching of low-side switches  $S_2$  and  $S_6$ . It takes 50 ms for the voltage of the gate driver to rise from zero to 16 V with a smoothing capacitor of the gate driver  $C_{out}$  of 20  $\mu\text{F}$ . After 50 ms from the start of the system, the proposed gate circuit operates stably. The starting time depends on the capacitance of the smoothing capacitor. It takes 160 ms when the capacitance  $C_{out}$  of the smoothing capacitor is 320  $\mu\text{F}$ . From Fig. 8, the proposed system does not need an additional circuit to help the start-up.

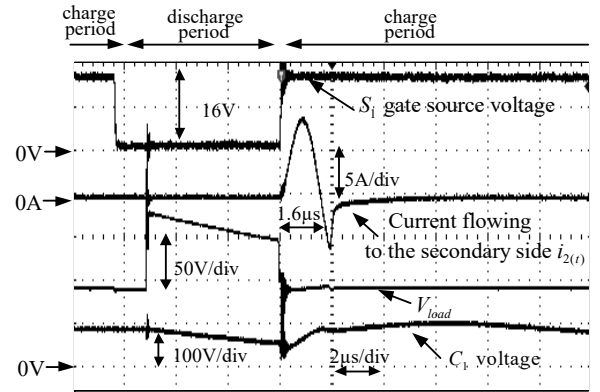
From the experimental results, GDU is driven by the proposed power supply method.

#### IV. CONCLUSIONS

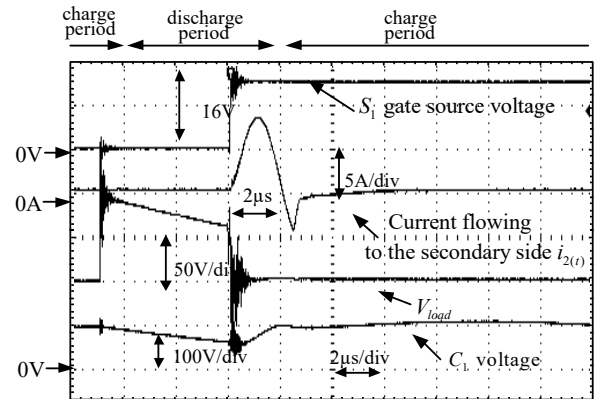
In this paper, an auxiliary power supply for the gate drive using a transformer during the charging operation of the Marx circuit has been proposed. First, the design of the transformer inserted into the proposed circuit is described in this paper. Then, we confirmed the validity of the design method of the system through simulations and experiments. The gate drive power of 1 W or more is supplied using the designed transformer. Therefore, it is found that the gate drive is performed without the additional DC-DC converter.

Moreover, the proposed system has an additional role as suppressing the rush current, which occurs during the charging operation of the Marx circuit. The proposed system supplies the power to the gate driver without an effect on the discharge operation of the Marx circuit. The rush current

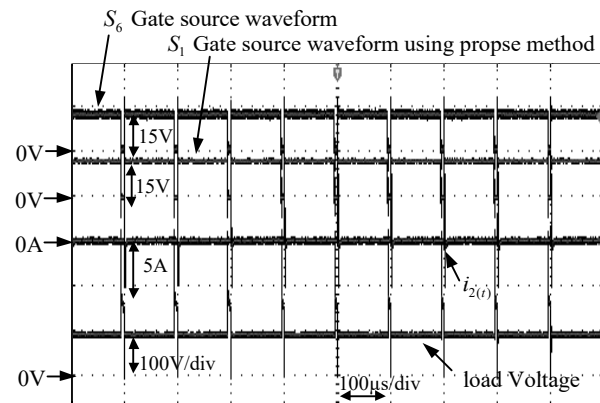
generated during the charging operation is suppressed with the proposed Marx circuit. It is confirmed that the rush current is suppressed by 75% as compared with the conventional configuration without the auxiliary power supply. As future plans, further suppression of rush current, experiments at rated load, and volume comparison will be performed.



(a) Operating waveform when a 10.5  $\mu\text{H}$  transformer is inserted



(b) Operating waveform when a 23.7  $\mu\text{H}$  transformer is inserted



(c) Gate signal waveform during stable operation and current waveform flowing on the secondary side of the transformer

Fig. 6. Experimental results in the proposed power supply method.

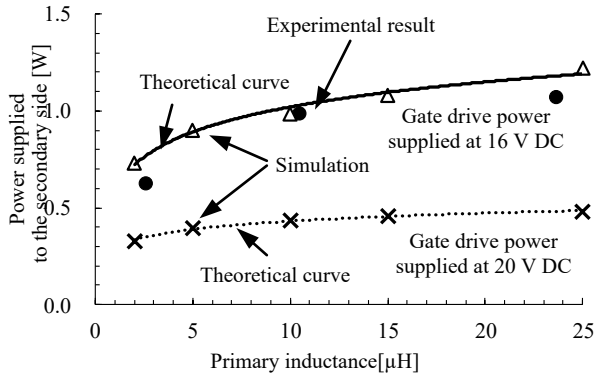


Fig. 7. Relationship between obtained power.

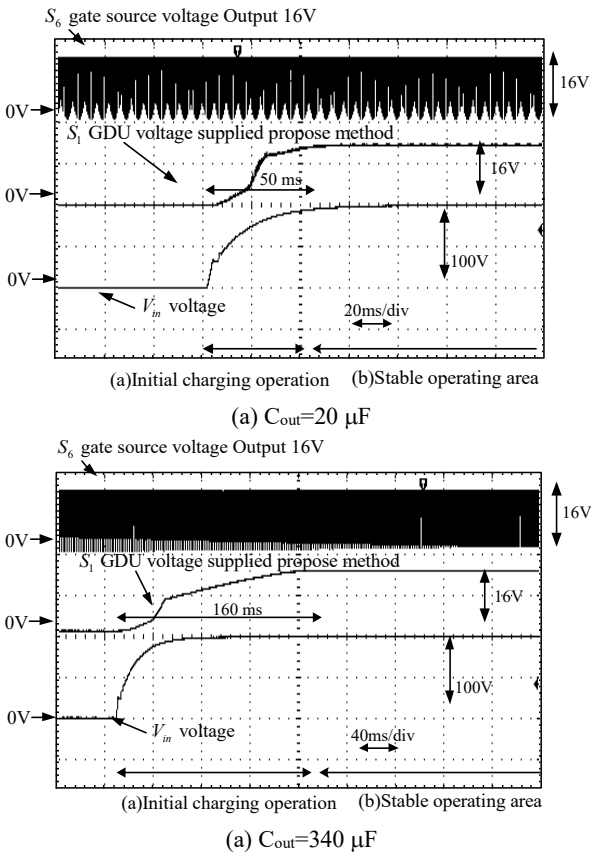


Fig. 9. Operation waveform from initial state.

## REFERENCES

- [1] Q. Zhao, S. Li, R. Cao, D. Wang and J. Yuan, "Design of Pulse Power Supply for High-Power Semiconductor Laser Diode Arrays," in IEEE Access, vol. 7, pp. 92805-92812, 2019
- [2] T. Sakamoto and H. Akiyama, "Solid-State Dual Marx Generator With a Short Pulsewidth," in IEEE Transactions on Plasma Science, vol. 41, no. 10, pp. 2649-2653, Oct. 2013
- [3] Y. Wang, K. Liu, J. Qiu and W. Dong, "A Stage-Stage Paralleled Topology of All-Solid-State Marx Generator for High Current," in IEEE Transactions on Plasma Science, vol. 47, no. 10, pp. 4488-4494, Oct. 2019
- [4] T. Sakamoto, A. Nami, M. Akiyama and H. Akiyama, "A Repetitive Solid State Marx-Type Pulsed Power Generator Using Multistage Switch-Capacitor Cells," in IEEE Transactions on Plasma Science, vol. 40, no. 10, pp. 2316-2321, Oct. 2012
- [5] C. Yao, S. Dong, Y. Zhao, Y. Mi and C. Li, "A Novel Configuration of Modular Bipolar Pulse Generator Topology Based on Marx Generator With Double Power Charging," in IEEE Transactions on Plasma Science, vol. 44, no. 10, pp. 1872-1878, Oct. 2016
- [6] J. Perez, T. Sugai, A. Tokuchi and W. Jiang, "Marx Generators Based on MOS-Gated Switches With Magnetic Assist for Accelerator Applications," in IEEE Transactions on Plasma Science, vol. 46, no. 6, pp. 2114-2119, June 2018
- [7] K. W. Lee et al., "Performance Analysis of a Short-Pulse Marx Generator for High-Power Relativistic Applications With a Solution Load," in IEEE Transactions on Plasma Science, vol. 43, no. 7, pp. 2174-2181, July 2015
- [8] S. Zabihi, Z. Zabihi and F. Zare, "A Solid-State Marx Generator With a Novel Configuration," in IEEE Transactions on Plasma Science, vol. 39, no. 8, pp. 1721-1728, Aug. 2011
- [9] Y. Achour, J. Starzyński and A. Lasica, "New Marx Generator Architecture With a Controllable Output Based on IGBTs," in IEEE Transactions on Plasma Science, vol. 45, no. 12, pp. 3271-3278, Dec. 2017
- [10] M. Taherian, M. Allahbakhshi, E. Farjah and H. Givi, "A Modular Topology of Marx Generator Using Buck-Boost Converter," in IEEE Transactions on Plasma Science, vol. 47, no. 1, pp. 549-558, Jan. 2019
- [11] M. Taherian, M. Allahbakhshi, E. Farjah and H. Givi, "An Efficient Structure of Marx Generator Using Buck-Boost Converter," in IEEE Transactions on Plasma Science, vol. 46, no. 1, pp. 117-126, Jan. 2018
- [12] Z. Li, H. Liu, J. Rao and S. Jiang, "Gate Driving Circuit for the All Solid-State Rectangular Marx Generator," in IEEE Transactions on Plasma Science, vol. 47, no. 8, pp. 4058-4063, Aug. 2019
- [13] Z. Li, H. Liu, S. Jiang and J. Rao, "A novel drive circuit with overcurrent protection for solid state pulse generators," in IEEE Transactions on Dielectrics and Electrical Insulation, vol. 26, no. 2, pp. 361-366, April 2019
- [14] J. Itoh, T. Kinomae, "Experimental Verification of a one-turn Transformer Power Supply Circuit for Gate Drive Unit", EPE-PEMC, No. T9, pp. 59-65 (2010)
- [15] Koji Orikawa, Takeshi Kinomae, and Jun-ichi Itoh "Experimental Verification of Self-Supplying Power Circuit using One-Turn Transformer for Gate Drive Unit," IEEJ J. Industry Applications, vol. 8, no. 1, pp. 12-22, 2019.
- [16] Hiroshi Shinoda, and Takahide Terada, "Insulated Signal Transmission System with Near-field Resonant Coupler to Drive High-voltage Power Devices", IEEJ J. Industry Applications, vol.6, no.3, pp. 205-212, 2017.
- [17] Koji Yamaguchi, Kenshiro Katsura, Tatsuro Yamada, Yukihiko Sato "Comprehensive Study on Gate Driver for SiC-MOSFETs with Gate Boost" IEEJ J. Industry Applications, vol. 7, no. 3, pp. 218-228, 2018.
- [18] Hiroshi Shinoda, and Takahide Terada, "Insulated Signal Transmission System with Near-field Resonant Coupler to Drive High-voltage Power Devices", IEEJ J. Industry Applications, vol.6, no.3, pp. 205-212, 2017.